Effects of Thickness Extension Mode Resonance Oscillation of Acoustic Waves on Catalytic and Surface Properties. II. Ethanol Decomposition on a Thin Pd Film Catalyst Deposited on Positively Polarized *z*-Cut $LiNbO_3$

Y. Yukawa, N. Saito, H. Nishiyama, and Y. Inoue*

Department of Chemistry, Nagaoka University of Technology, Nagaoka 940-2188, Japan

Received: April 25, 2002; In Final Form: July 23, 2002

The effects of thickness extension mode resonance oscillation (TERO) of acoustic waves on the catalytic properties of a 100 nm thick Pd film deposited a positively polarized ferroelectric *z*-cut $LiNbO_3$ single crystal were studied. For ethylene and acetaldehyde production in ethanol decomposition, the TERO accelerated ethylene production only and enhanced the selectivity for ethylene production from 40% to 96%. Randomly distributed standing waves due to large lattice displacement vertical to the surface were generated with TERO on. The photoelectron emission spectra showed that the TERO caused a positive shift of the threshold energy of photoelectron emission from a Pd surface, indicating an increase in the work function of the surface. The TERO effects on a Pd catalyst were compared with those previously observed for a Ag catalyst.

Introduction

The resonance oscillation (RO) of bulk acoustic waves can be generated by applying rf electric power to the electrodes attached to the front and rear planes of a ferroelectric crystal.[1,2] In recent studies of RO effects on heterogeneous catalysis, we have demonstrated the roles of lattice vibration modes due to RO in catalytic activity.[3−11] The thickness extension mode resonance oscillation (TERO) generated on a *z*-cut $LiNbO_3$ (referred to as *z*-LN) single crystal and the thickness shear mode resonance oscillation (TSRO) on an *x*-cut $LiNbO_3$ (*x*-LN) crystal were applied to ethanol decomposition over a thin Ag film catalyst deposited on the crystals. The TERO with lattice vibration vertical to the surface enhanced ethylene production without a significant change in acetaldehyde production, exhibiting remarkable ability to increase the selectivity for ethylene production. On the other hand, the TSRO with lattice displacement parallel to the surface caused activity enhancement for neither ethylene nor acetaldehyde production.[4] These results have clearly shown that the vertical lattice vibration plays a decisive role in catalyst activation.

Because a *z*-LN ferroelectric crystal employed for TERO has spontaneous polarization normal to the surface, it exposes a positively polarized surface on one plane and a negatively polarized surface on the opposite plane. The influences of polarized surfaces on the TERO-induced catalyst activation are one of the important factors to be examined. Very recently,[12] we have fabricated a catalyst in which a thin Ag film was deposited on the positively polarized surface of *z*-LN only and used it for ethanol decomposition. The TERO effects on the Ag catalyst were found to be larger compared with those on a Ag catalyst deposited on positive and negatively polarized surfaces of the same substrate. These results suggest that the TERO effects depend on the polarized surfaces. It is important to confirm whether the influences of polarized surfaces on TERO-induced catalyst activation exist in different kinds of metal catalysts. In the present work, a Pd metal, being a d-metal, was deposited on a positively polarized *z*-LN surface and its catalytic properties for ethanol decomposition were investigated in detail in the absence and presence of TERO. The magnitude of vertical lattice displacements with TERO was analyzed by means of a 3-D laser Doppler method. Furthermore, changes in electronic structures with TERO were measured by a photoelectron emission spectroscopic method. The results obtained were compared with those for a Ag catalyst.

Experimental Sections

A poled ferroelectric single-crystal substrate of *z*-LN was the same as that used previously.[12] A thin Pd catalyst film was deposited at a thickness of 100 nm on a positively polarized surface of the crystal by the resistance heating of pure Pd metal in a vacuum. The back plane of the negatively polarized surface was covered with a thin Au film that was used as an electrode only. The catalytic activity of the Au electrode was negligible compared to that of a Pd catalyst. The catalyst was denoted here as (+)Pd.

Catalytic ethanol decomposition, that is, dehydrogenation to produce acetaldehyde and dehydration to ethylene, was performed in a fashion similar to that previously employed. Briefly, ethanol vapor of 2.7−4.0 kPa was introduced to a closed gas circulation apparatus, and reactants and products were analyzed by an on-line gas chromatograph. Selectivity for ethylene production was defined as a percentage of the amount of ethylene production to the total amount of ethylene and acetaldehyde production. For the generation of TERO, an electric signal from a network analyzer (Anritsu MS3606B) was amplified (Kalmus, 250FC) and applied to a catalyst sample after impedance adjustment. As shown previously, the TERO of *z*-LN provided a series of resonance frequencies of 3.5, 10.5, 17.4, and 24.1 MHz. The primary resonance frequency of 3.5 MHz was used in the present study. The temperature of the catalyst surface was measured by shifts in the resonance frequency and was kept constant during reaction by using an outer electric furnace as described elsewhere.

Lattice displacement caused by TERO was recorded as 3-D images using a homemade laser Doppler apparatus as described previously.[8] A He−Ne laser beam reflected from a Pd catalyst

10.1021/jp021054t CCC: $22.00 © 2002 American Chemical Society
Published on Web 09/05/2002

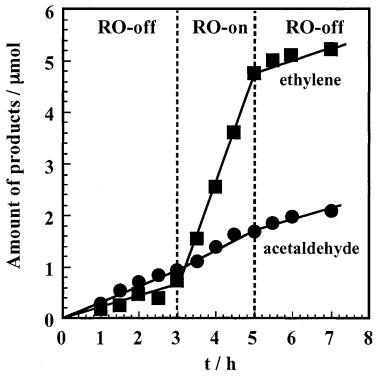

Figure 1. Changes in (■) ethylene and (●) acetaldehyde production in ethanol decomposition on (+)Pd with TERO on and TERO off: rf power, $J = 3$ W; reaction temperature, $T_r = 603$ K; ethanol pressure, $P_e = 4.0$ kPa.

surface on a sample stage movable for the *x* and *y* directions was monitored by a vibrometer (Ono Sokki LV-1300).

Photoelectron emission spectra of a Pd surface were measured in air by a low-energy photoelectron spectroscopic method.[3] A Pd surface was irradiated with monochromatized deuterium lamp light, and the number of emitted photoelectrons was plotted against photon energy. The threshold energy for photoelectron emission was measured within an accuracy of 0.01 eV and compared with TERO off and TERO on.

Results

In ethanol decomposition on a Pd catalyst, ethylene and acetaldehyde were simultaneously produced in the gas phase nearly proportionally to the reaction time. Figure 1 shows changes in the production of ethylene and acetaldehyde with TERO on and TERO off. With TERO on at 3 W, an immediate increase in ethylene production occurred. On the other hand, no significant changes in the production of acetaldehyde were observed with TERO on. The TERO effects on ethylene production were reversible: enhanced production decreased to the original low level with TERO off. Ethanol consumption was 1.2% in the 7 h reaction. The reaction behavior with TERO on and off was quite analogous to that observed for (+)Ag.[12]

Figure 2 shows the temperature dependence of the reaction in the temperature range 593−633 K. The ethylene production provided the activation energy of 127 kJ mol^{-1} without TERO. With TERO on, the temperature dependence became smaller and the activation energy decreased to 98 kJ mol^{-1}. The activation energy for acetaldehyde production was 81 kJ mol^{-1} and remained unchanged with TERO on.

Figure 3 shows the pressure dependence of ethylene production at 593 K. The reaction order, *n*, with respect to ethanol pressure, P_e, was 0.1. With TERO on at 3 W, pressure dependence was slightly larger and the value of *n* increased to 0.2. The same pressure dependence was observed for acetaldehyde production.

Figure 4 shows the catalytic activity for ethylene and acetaldehyde production as a function of rf power introduced to a Pd catalyst. The activity enhancement for ethylene production was small in a low rf power region of <2 W and became significant at around 3 W. With increasing power, a steep rise of the activity occurred. In contrast, the activity for acetaldehyde production was small even at a high-power region. Figure 4 also shows selectivity for ethylene production as a function of power. The selectivity was 40% with TERO off,

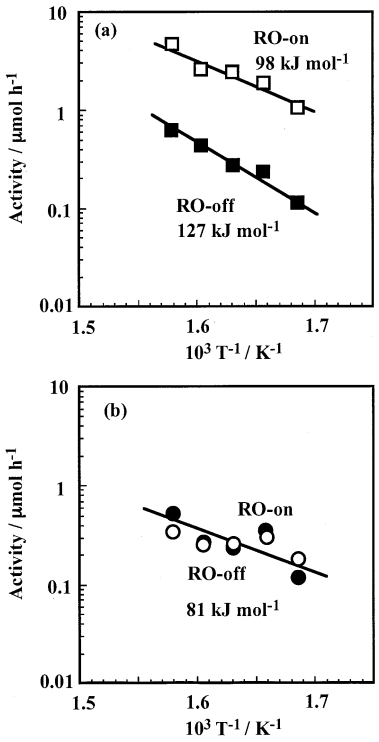

Figure 2. Temperature dependence of (a) ethylene and (b) acetaldehyde production in ethanol decomposition with (■, ●) TERO off and (□, ○) TERO on: $J = 3$ W; $P_e = 4.0$ kPa.

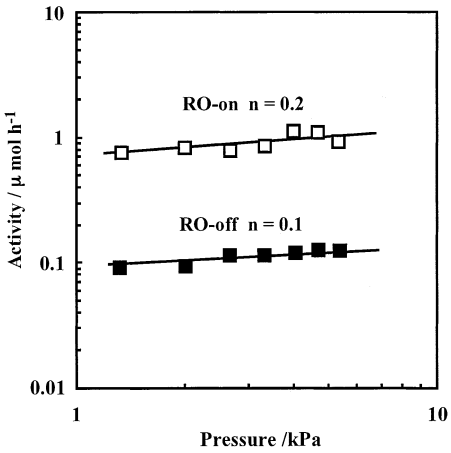

Figure 3. Pressure dependence of (a) ethylene and (b) acetaldehyde production in ethanol decomposition with (■) TERO off and (□) TERO on: $J = 3$ W; $T_r = 593$ K.

increased monotonically with increasing power, and was attained at 96% at 4.5 W.

Figure 5 shows the 3-D images of standing waves formed by TERO at different power levels. At 1 W, standing waves normal to the surface appeared clearly over a Pd surface. The magnitudes of the waves were considerably different. With increasing power, the waves became remarkably large. The magnitude of the wave represents periodic lattice displacement vertical to the surface. Figure 6 shows the distribution of lattice displacements at 1, 3, and 5 W. The distribution provided a peak with a maximum, for which one can define three parameters such as maximum lattice displacement, L_{max}, average lattice displacement, L_{av}, and a full width at half-maximum (fwhm) of peak. At 1 W, L_{max} and L_{av} were 31 and 9 nm, respectively. The value of fwhm was as narrow as 11 nm. At 3 W, L_{max} increased to 49 nm and L_{av} to 16 nm. The lattice

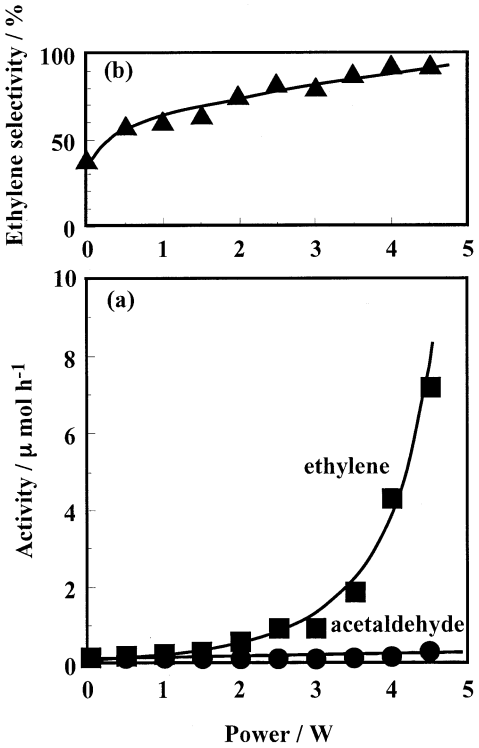

Figure 4. Changes in catalytic activity and selectivity with rf power: (■) activity for ethylene production; (●) activity for acetaldehyde production; (▲) selectivity for ethylene production. $T_r = 583$ K; $P_e = 4.0$ kPa.

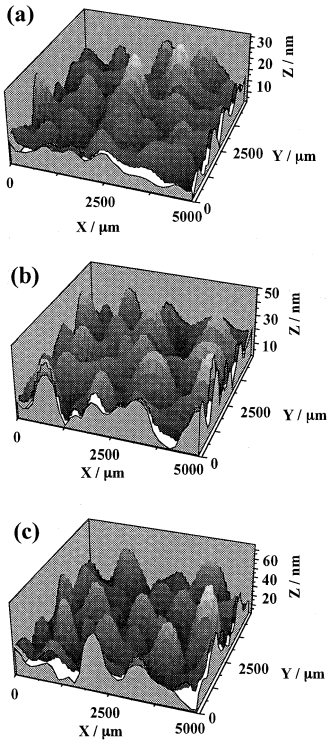

Figure 5. Three-dimensional images of standing waves observed by laser Doppler measurements: (a) $J = 1$ W; (b) $J = 3$ W; (c) $J = 5$ W. Temperature of measurements, T_m = room temperature.

displacement distribution became broader: the fwhm was 20 nm. At 5 W, L_{max} reached 75 nm and the fwhm was as broad as 24 nm. As a result of these changes, the maximum position of the curves shifted toward larger lattice displacement with increasing power. Figure 7 shows lattice displacements as a

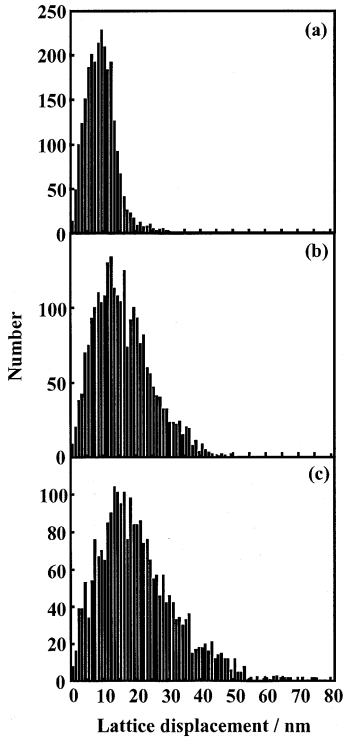

Figure 6. Distributions of lattice displacement as a function of rf power: (a) $J = 1$ W; (b) $J = 3$ W; (c) $J = 5$ W. T_m = room temperature.

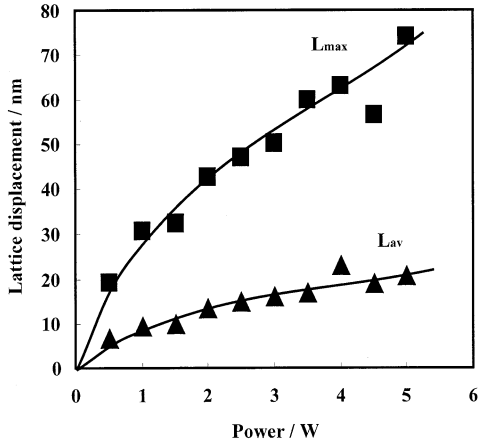

Figure 7. Changes in maximum (L_{max}) and average (L_{av}) lattice displacements with increasing rf power.

function of rf power. With increasing power, L_{max} and L_{av} enhanced considerably up to 1.5 W, followed by gradual increases.

Figure 8 shows photoelectron emission spectra from a Pd surface with TERO off and TERO on. With TERO off, the photoelectron emission was not observed below 4.78 eV. Significant electron emission started at around 4.80 eV, and from the extrapolation of electron emission line, the threshold energy was evaluated to be 4.83 eV. In the presence of TERO at 1 W, an electron emission pattern shifted toward higher photon energy by 0.02 eV. At 3 W, the shift became significant and the threshold energy increased by 0.07 eV. At 5 W, another shift occurred and the threshold energy increased by as much as 0.12 eV. Figure 9 shows the threshold energy shift as a function of rf power. The shift increased nearly proportionally to rf power up to 5 W. Figure 10 shows correlation between the work function shifts and the activity changes in ethylene

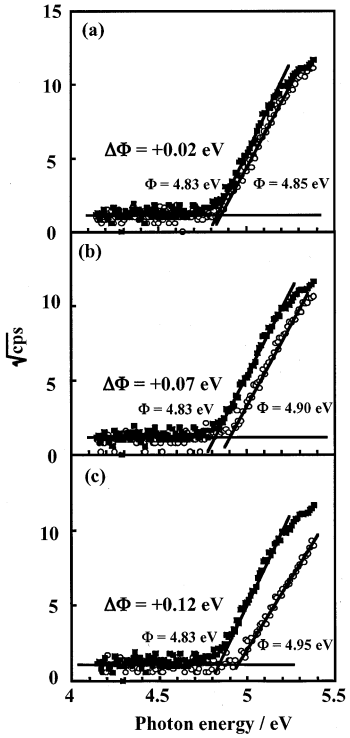

Figure 8. Photoelectron emission spectra of (+)Pd with (■) TERO off and (○) TERO on: (a) $J = 1$ W; (b) $J = 3$ W; (c) $J = 5$ W. T_m = room temperature.

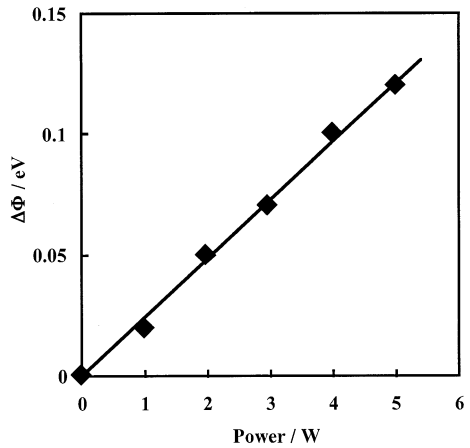

Figure 9. A shift of the threshold energy with rf power.

production. The catalytic activity increased gradually with increasing work function and steeply at above 0.07 eV.

Discussion

The TERO caused a dramatic enhancement of the catalytic activity of (+)Pd for ethylene production but not for acetaldehyde production, exhibiting a remarkable increase in the selectivity for ethylene production. The changes in reaction behavior were characteristic of the TERO effects and were analogous to those observed for (+)Ag,[12] indicating that the TERO has similar effects on different kinds of the metals. However, there are some differences in the extent of the TERO effects between (+)Pd and (+)Ag. At 3 W, a change in the activation energy for ethylene production on (+)Ag was from 156 to 103 kJ mol^{-1},whereas that on (+)Pd was from 127 to 98 kJ mol^{-1}. The extent of activation energy decrease was 50% larger for (+)Ag than that for (+)Pd.

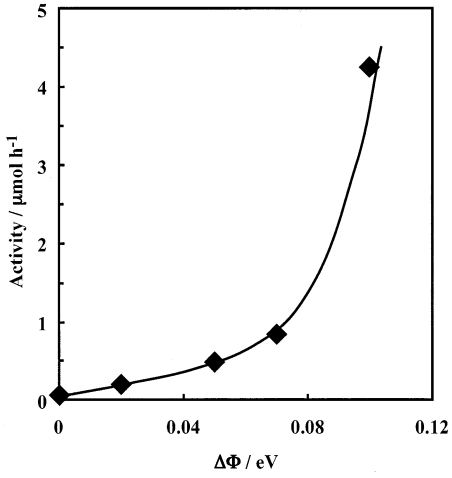

Figure 10. Correlation between the work function shift and the catalytic activity for ethylene production.

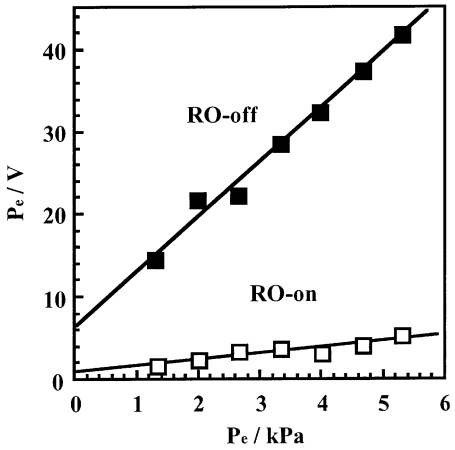

Figure 11. Plots of P_e/V and P_e.

The pressure dependence showed that the reaction order with respect to ethanol pressure was 0.1 with TERO off and increased to 0.2 with TERO on. Provided that the rate-determining step is the decomposition of adsorbed ethanol, the reaction rate, V, is given by

$$V = k\theta = kKP_e/(1 + KP_e) \quad (1)$$

where k is the rate constant, θ is the surface coverage of ethanol, and K is the equilibrium constant of ethanol adsorption. This equation can be converted to

$$P_e/V = P_e/k + 1/(kK) \quad (2)$$

As shown in Figure 11, the plot of P_e/V vs P_e showed good linear relations with both TERO on and TERO off, indicating that the decomposition of strongly adsorbed[13] and fully surface-covering ethanol is the rate-determining step. From the slope and y-axis, the value of K was calculated to be 1.0 kPa^{-1} with TERO off and 0.8 kPa^{-1} with TERO on. A decrease in K value indicates that the adsorption of ethanol on (+)Pd became weaker in the presence of TERO. This is consistent with the previous conclusion obtained in a kinetic study of ethanol oxidation over (+)Pd.[9]

The 3-D images of standing waves observed in laser Doppler measurements exhibited periodic lattice displacement on the Pd surface with TERO on. The important features are that the lattice displacement was vertical to the Pd surface and also that the magnitude of vertical lattice displacement increased remarkably

with increasing power: L_{max} was 31 nm at 1 W, 49 nm at 3 W, and 75 nm at 5 W. Under the same rf power conditions, L_{max} of (+)Ag was 38 nm at 1 W and 63 nm at 3 W. Lattice displacement was 20% smaller for (+)Pd than for (+)Ag.

As shown in Figure 8, the TERO caused a positive shift of the threshold energy of photoelectron emission from a (+)Pd surface, indicating that the work function of the Pd surface increased with TERO on. The work function shifted in an almost linear fashion with increasing rf power; the shift was 0.07 eV at 3 W. In comparison with the results for (+)Ag, the positive shift of the work function was the same, whereas the extent of work function change at 3 W was 50% smaller for (+)Pd than for (+)Ag.

By assuming uniform lattice atom expansion, we calculated a change in surface atom−atom distance due to the largest lattice displacement to be less than 10^{-5}%.[14] Thus, it is unlikely that the geometric site effects relating to bond lengthening or shortening of surface atoms are directly responsible for work function shifts. As discussed previously according to a jellium model,[15,16] the enhancement of the work function of a metal is associated with an increase in the density of electrons that spill out from the topmost surface atom layer, because the density controls the magnitude of an energy barrier due to an electric dipole layer at the surface. We have explained the enhancement of the work function on the basis of an assumption that the vertical lattice displacement has an influence on the density of spilled-out electrons. This assumption can be verified by the fact that the work function increases in Ag and Pd were induced only with TERO having vertical lattice displacement but not with TSRO having a small component of vertical lattice displacement. Namely, for changes in the work function, it is essential that the direction of lattice displacement is consistent with the direction toward which electrons spill out. This consideration suggests that larger vertical lattice displacement could lead to larger shift of work function. The fact that the extent of work function shift was larger for (+)Ag, which had larger lattice displacement compared to (+)Pd, is in line with this view. As differences in TERO effects between (+)Pd and (+)Ag, the TERO on Pd caused a decrease in the reaction order with ethanol pressure, that is, weaker adsorption of ethanol, whereas no significant variations of the reaction order were induced for Ag. Thus, the TERO has larger effects on the adsorption of ethanol for Pd than for Ag. Because the work function shifts of Pd were smaller than those of Ag, the influence of work function changes on the adsorbed state is considered to be larger for Pd. This suggests that the TERO has larger suppressing effects of back-donation to the adsorbed ethanol on Pd than those on Ag.

Figure 10 shows correlation between the catalytic activity enhancement and the work function shift. The activity increased gradually and steeply with increasing work function, indicating that the work function increases are responsible for the catalyst activation for ethanol decomposition.

The enhancement of ethylene selectivity with the TERO is explained in terms of a change in the adsorbed structure of ethanol, as discussed previously.[12] The strong adsorption is formed by electron transfer from a metal atom to an oxygen atom of adsorbed ethanol (electron back-donation). Increases in work function with TERO on lower the ability of back-donation, leading to weak bond formation between the adsorbed ethanol and the Pd surface.[17,18] Because the formation of a molecularly chemisorbed ethanol rather than an ethoxy species is favored under weak interactions, an increase in work function with TERO on promotes the conversion of the ethoxy species to the molecularly chemisorbed ethanol on the Pd surface. The orientation of adsorbed ethanol species to the surface is dependent on the conditions of the chemisorbed ethanol species. In a molecularly chemisorbed ethanol, the O−H bond was oriented parallel to the surface, whereas the C−C bond is oriented perpendicular to the surface in an ethoxy species.[19] Because of easier access of β-H and OH group to the metal surface, the molecularly chemisorbed ethanol is likely to undergo the abstraction of HOH groups, which leads to the formation of ethylene. The structural view accounts for the TERO effects that enhance the selectivity for ethylene production.

In conclusion, the TERO effects on the reaction selectivity have been demonstrated to be useful for (+)Pd and proposed to be due to similar mechanism proposed for (+)Ag. Changes in the work function of a (+)Pd surface with dynamic vertical lattice displacement are responsible for the effects.

Acknowledgment. This work was supported by a Grant-in-Aid for Scientific Research (B) from The Ministry of Education, Science, Sports and Culture.

References and Notes

(1) Auld, B. A. *Acoustic Fields and Waves in Solids*; Wiley & Sons: New York, 1973; Vol. 2.
(2) Ikeda, T. *Fundamentals of Piezoelectricity*; Oxford University Press: New York, 1990; p 117.
(3) Ohkawara, Y.; Saito, N.; Inoue, Y. *Chem. Phys. Lett.* **1998**, *286*, 502.
(4) Saito, N.; Inoue, Y. *J. Chem. Phys*. **2000**, *113*, 469.
(5) Saito, N.; Nishiyama, H.; Sato, K.; Inoue, Y. *Surf. Sci*. **2000**, *454/456*, 1099.
(6) Saito, N.; Nishiyama, H.; Inoue, Y. *Appl. Surf. Sci*. **2001**, *169/170*, 259.
(7) Inoue, Y. *Catal. Surv. Jpn.* **1999**, *3* , 95.
(8) Saito, N.; Nishiyama, H.; Sato, K.; Inoue, Y. *Chem. Phys. Lett*. **1998**, *297*, 72.
(9) Saito, N.; Sato, K.; Inoue, Y. *Surf. Sci*. **1998**, *417*, 384.
(10) Saito, N.; Sakamoto, M.; Nishiyama, H.; Inoue, Y. *Chem Phys. Lett*. **2001**, *341*, 232.
(11) Saito, N.; Nishiyama, H.; Sato, K.; Inoue, Y. *Solid State Ionics*, **2000**, *136/137*, 819.
(12) Saito, N.; Inoue, Y. *J. Phys. Chem. B* **2002**, *106*, 5011.
(13) Sexton, B. A.; Rendukic, K. D.; Hughes, A. E. *Surf. Sci*. **1982**, *121*, 181.
(14) Nishiyama, H.; Saito, N.; Izumi, K.; Inoue, Y. *J. Phys. Chem. B* **2002**, *106*, 6538.
(15) Lang, N. D.; Kohn, W. *Phys. Rev*. **1970**, *B1*, 4555.
(16) Smith, J. R. *Phys. Rev*. **1969**, *181*, 522.
(17) Marcel, R. I. *Principles of Adsorption and Reactions on Solid Surfaces*; Wiley & Sons: New York, 1996.
(18) Somorjai, G. *Introduction to Surface Chemistry and Catalysis*; Wiley & Sons: New York, 1994.
(19) Kratochwil, Th.; Wittmann M.; Küppers, J. *J. Electron. Spectrosc. Relat. Phenom*. **1993**, *64/65*, 609.